DOI: 10.24996/ijs.2023.64.9.18

ISSN: 0067-2904

Reservoir Characteristics for Khasib Formation in selected wells of East Baghdad Oil field, Iraq

Israa Qasem Hussain Tukkee, Salah Ali Hussain*, Abdalratha Mohammed Sahaab
Department of Petroleum Geology and Minerals, College of Science, University of Diyala. Diyala, Iraq

Received: 14/8/2022 Accepted: 9/1/2023 Published: 30/9/2023

Abstract

Four subsurface sections and electrical, porosity logs, and gamma-ray logs of the Khasib Formation (age Late Turonian-Lower Coniacian) were studied to identify reservoir characteristics and to evaluate the reservoir properties of the Khasib reservoir units in the East Baghdad oilfield. The lithology of the formation is limestone throughout the whole sequence in all studied wells EB-83, EB-87, EB-92, and EB94. It is bounded conformably from the top by Tanuma Formation and has a conformable lower contact with Kifl Formation. The lower and upper boundaries of the formation were determined using well log analysis, and the formation was divided into three main rock units (Kh1, Kh2, and Kh3), depending on the porosity logs. The porosity was calculated using acoustic or sonic, neutron, and density logs. The effective porosity (average 0.0 - 0.32 %) is the predominant porosity in the formation and to less extent; the secondary porosity. The volume of shale is very low (average 0.0 - 0.13 %), indicating limestone is the main rock of the Khasib Formation. The study of the reservoir water (average 0.11- 1.0%) and hydrocarbon saturations (average 0.0 - 0.88 %) showed that the formation contains varying proportions and quantities of water and hydrocarbons suspended in the wall void, and hydrocarbons capable of being produced. The lithological study reflected that the predominant lithic formation is limestone. It was found that Kh 2 unit is the best oil reservoir unit in all selected wells in terms of porosity, water saturation, diagenesis processes, and microfacies analysis.

Keywords: Reservoir Characteristics; Khasib Formation; East Baghdad Oilfield; Volume Shale; Porosity; Water Saturation.

الخصائص المكمنية لتكوين الخصيب في ابار مختارة لحقل شرق بغداد النفطي, العراق.

اسراء قاسم حسين تكي, صلاح علي حسين*, عبد الرضا محمد سحاب
قسم جيولوجيا النفط والمعادن, كلية العلوم, جامعة ديالى, العراق

الخلاصة

تمت دراسة اربعة ابار وتحليل المجسات الكهربائية و المسامية ومجسات اشعة كاما لتكوين الخصيب (التوروني المتأخر – كونياسيان المبكر) لتحديد خواصة وصفاتة المكمنية في حقل شرق بغداد النفطي. صخارية التكوين هي الحجر الجيري في جميع التتابعات العائدة للابار
(EB-83, EB-87, EB-92, EB-94). يحده من الاعلى تكوين تنومة ويكون بحد توافقي معه، كذلك فان الحد الاسفل للتكوين يكون متوافقا مع تكوين الكفل . تم تحديد الحدود السفلية والعلوية للتكوين بأستخدام

*Email: salahpgm@yahoo.com

المجسات الكهربائية والمسامية ومجس اشعة كاما، كما تم تقسيم التكوين الى ثلاثة وحدات صخرية رئيسية (Kh1, Kh2, and Kh3) اعتمادا على مجسات المسامية. حسبت المسامية بأستخدام مجساتها (الصوتي والنيوتروني والكثافة) واتضح ان المسامية الفعالة (بمعدل (%0 −0.32) :هي المسامية الغالبة في التكوين وان المسامية الثانوية قليلة جدا. اما بالنسبة للحجم السجيلي ايضا قليل جدا (بمعدل: (0.13− 0) %) تعكس ان صخارية تكوين الخصيب هي الحجر الجيري. بينت الدراسة المكمنية للتشبعات المائية (بمعدل: (1_ 0.11) %) والهيدروكاربونية (بمعدل: (0.88_ 0) %) ان التكوين يحتوي على نسب وكميات متفاوتة من الماء والهيدروكاربونات العالقة بجدار الفراغات والهيدروكاربونات القابلة للانتاج. كما اظهرت دراسة الصخارية ان الصخارية الغالبة للتكوين هي الحجر الجيري وان الوحدة Kh 2 هي أفضل وحدة مكمنية نفطية في جميع الآبار المختارة من حيث المسامية ، وتشبع المائي ، والعمليات التحويرية ، وتحليل السحني الدقيق.

1. Introduction

Khasib Formation (age Late Turonian-Lower Coniacian) was first introduced by Bellen,et al, (1959) [1] in well Zubair-3, which is located between the excavated depths (2146.3- 2196.3 m) and a thickness of 50 m. The upper part of dark fine-grained marly limestone of 29 m thickness and the lower part of alternates dark and greenish shales and dark limestone of 21 m thickness. The fossils contents are *Globigerina sp.*, *Gumbelina spp*., and *Oligostegina*. The underlying Khasib formation is the Kifil Formation; contact is conformable, the overlying formation is Tanuma Formation; contact is conformable in a change of black, fissile shales above to grey marly limestones below [1].

1.1 Aims of Study

1. Identifying reservoir characteristics of Khasib units by well-log interpretation.
2. Evaluation of the reservoir properties of the Khasib reservoir units.

1.2 Location of the Study Area

The study area is located in the East Baghdad oil field, (Figure 1). Four wells were selected, which are (EB-83, EB-87, EB-92, and EB-94) (Figure 1 and Table 1).

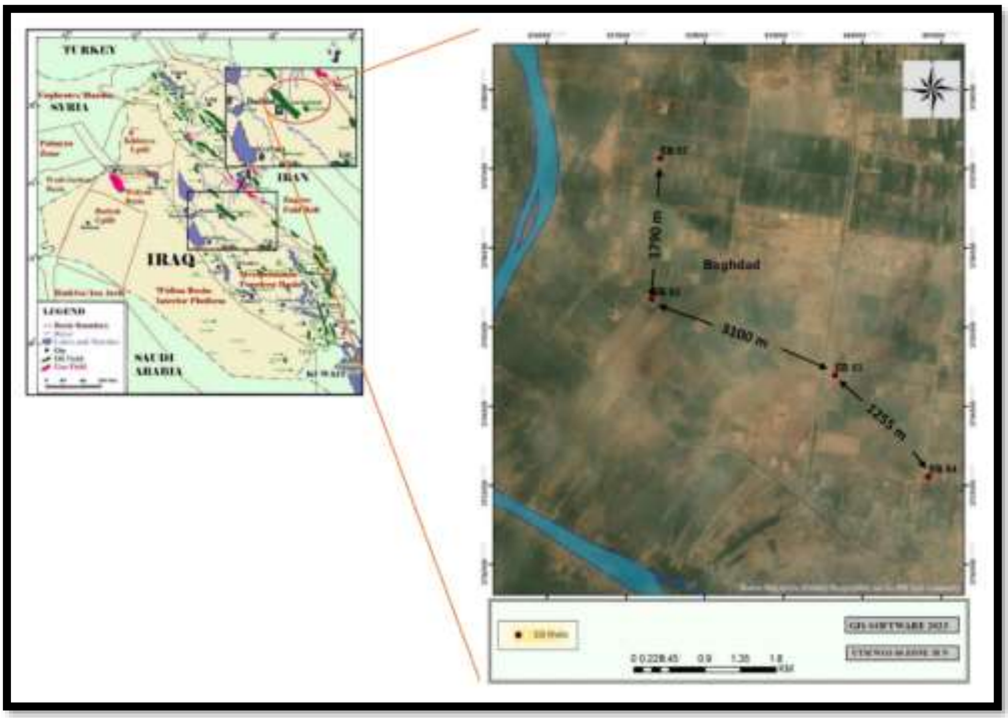

Figure 1: Location map of the study area.

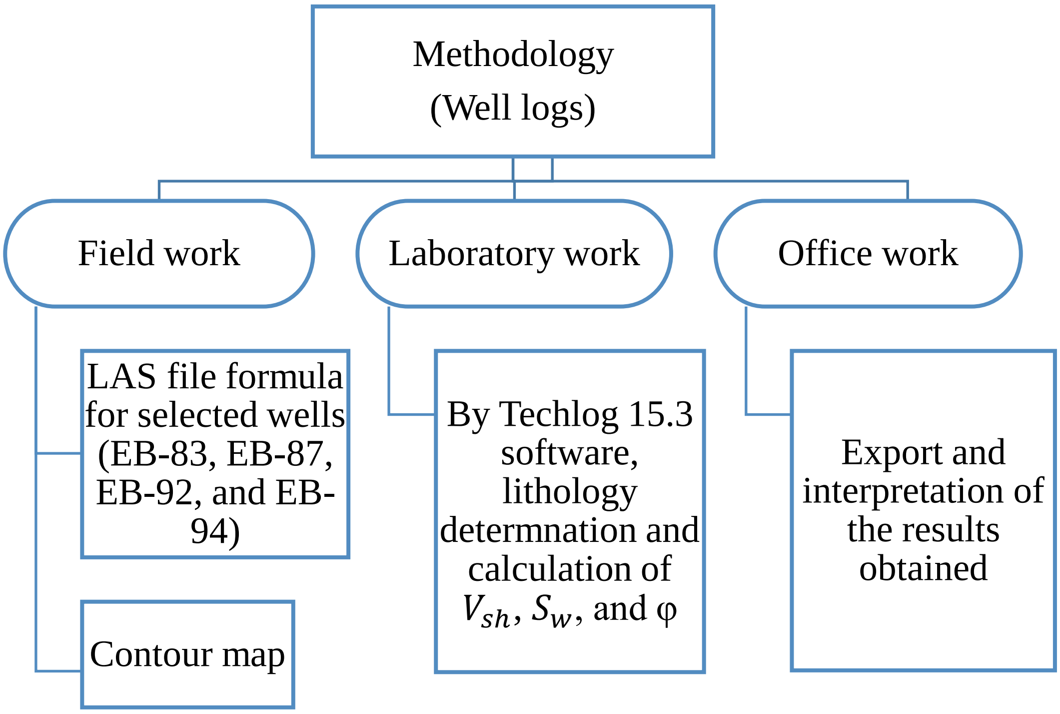

Table 1: The coordinates of the study wells with the upper limit and the thickness of Khasib formation

Well NO.	Depth (m)	Thickness (m)	X	Y
EB-83	(2148_ 2252.5)	104.5	33 28’ 29.25’’	44 21’ 12.86’’
EB-87	(2151.39_ 2253.15)	101.76	33 29’ 57.78’’	44 19’ 46.69”
EB-92	(2139.5_ 2241.17)	101.67	33 28’ 59.78’’	44 19’ 42.74”
EB-94	(2165.49_ 2264.5)	99.01	33 27’ 47.86’’	44 21’ 59.27’’

2. Methodology

Four subsurface sections selected from the wells of the East Baghdad oil field in the middle of Iraq, including EB-83, EB-87, EB-92, and EB-94) were studied. The well logs such as electrical, porosity logs, and gamma-ray logs are conducted to identify the reservoir characteristics and to evaluate the petrophysical properties represented by porosity, permeability, and water saturation of the Khasib reservoir units in the East Baghdad oilfield. The methodology adopted is explained in the steps presented in Flowchart 1. Techlog 15.3 software and Microsoft Excel are used to calculate the reservoir characteristics. The data were taken in LAS file format for four wells (EB-83, EB-87, EB-92, and EB-94) from Midline Oil Company.

Flowchart 1- Well logs methodology.

3. Result and Discussions

This study is one of the significant investigations through which some petrophysical properties are determined, represented by porosity, permeability, and water saturation. The volume of shale was calculated using gamma-ray logs and porosity logs (density log, neutron log, and the sonic or acoustic log) to determine the porosity of all types (effective and secondary). The process of interpreting the results was done through direct readings or through the application of the relationships and profiles set in finding the most important lithological and petrophysical properties of Khasib Formation (Flowchart 1).

3.1 Well Logs Analysis

The Well Logs Analysis includes direct interpretations of the results, measured from the selected well logs, such as the stratigraphic boundaries, determining the types of porosity, water, and hydrocarbon saturation.

3.1.1 Stratigraphic Boundaries

The Well Logs Analysis is used to determine the upper and lower boundaries of Khasib Formation. The behavior of the well logs is investigated using:

1. Gamma-ray log (GR Log)

The gamma-ray log is used to calculate the natural radiation emissions from the formation [2]. Most carbonate rocks contain natural radiation in varying quantities. These rays are emitted from the elements Potassium (K), Thorium (Th), and Uranium (U) and may be emitted from some fluids inside the rocks, which contain some dissolved elements.

The volume of shale was calculated from the gamma-ray log, equation (1) was used to calculate the gamma-ray coefficient, then to calculate the volume of shale [3]:

$$I_{GR} = \frac{(GR_{log} - GR_{min})}{(GR_{max} - GR_{min})} \qquad \text{……………………. (1).}$$

$\boldsymbol{I_{GR}}$**:** Gamma-ray index.

$\boldsymbol{GR_{log}}$**:** A gamma-ray reading by log*(API).*

$\boldsymbol{GR_{min}}$**:** Minimum value for a gamma-ray log (clean sand or carbonate).

$\boldsymbol{GR_{max}}$**:** Maximum value for a gamma-ray log (shale).

After extracting the gamma-ray coefficient, the volume of shale is calculated using equation (2) [4], (Figures 2, 3, 4 and 5):

$$V_{sh} = 0.33\ (2^{(2*I_{GR})} - 1)\ldots\ldots \qquad \text{………… (2).}$$

$\boldsymbol{V_{sh}}$**:** The volume of shale.

The result shows that the shale content is very low in all parts of the formation. This could be due to a curved gamma ray log that registers a gradual deflection of less than 20 API.

2. Electrical logs

In order to calculate the water saturationS_W, the formation water resistivity has to be known [5]. There are two methods to study the electrical resistance of sections from the subsurface layers, Deep laterolog (LLD), and microspherical laterolog (MSFL), (Figures 2, 3, 4, and 5). The principle of these logs depends mainly on the transmission of electric current through two electrodes on the surface of the earth and near the borehole. The difference in potential results is recorded using Ohm's law to receive the particular resistance. The presence of electrical conductivity in both mud and water and reservoir water is reversed by resistivity log data.

The result reflects that the reading rate (LLD) in the upper part of the formation (Kh1) is medium which is evidence of the presence of oil, while in the middle and lower parts (Kh 2 and Kh3) are low to medium to indicate the presence of hydrocarbons and water. The curve (MSFL) is reading medium resistance throughout Khasib Formation in all studied wells.

3.1.2 Porosity logs

Porosity is the first of the two basic characteristics of the reservoir (porosity and permeability). It can be expressed as the ratio of the volume of voids to the total volume of the rock as a percentage porosity (eq. 3) is usually denoted by the Greek letter phi (φ):

$$Porosity\ (\%) = \frac{Volume\ of\ voids}{Total\ volume\ of\ rock}\ x\ 100 \ldots \qquad \ldots\ldots\ldots\ldots (3)$$

Porosity logs (density log, neutron log, and sonic or acoustic log) are used, through which the effective porosity and secondary porosity can be calculated.

(1)Density log (RHOB Log)

A density log is one of the types of logs that measure porosity by measuring the formation electron density, which correlates with the total density ρ_b. The device consists of a radiation source that emits gamma rays into the formation and one or more detector receivers at a specific distance from the source. The emitted gamma rays collide with the electrons in the formation, leading to a loss in energy. Even though some energy is lost during the formation, the energy that is received by the recipient is counted as a measure of the formation density [6]. If the material has a high density, then most of the gamma rays will be absorbed by the material and a small percentage of it will reach the detector and be recorded [7]. This log's ability to identify gas-bearing areas and measure hydrocarbon density is one of its most crucial uses [2].

It is clear from [8] that the porosity calculations are not affected by the presence of hydrocarbons in reservoir rocks with low to medium porosity, but they are affected in rocks with high porosity, especially when saturated with gaseous hydrocarbons. The density log-derived porosity was calculated for Khasib Formation using Wiley's equation (4) [9], (Figures 2,3,4 and 5).

$$\varphi_D = \frac{\rho_{ma}-\rho_b}{\rho_{ma}-\rho_f} \ldots \qquad \ldots\ldots\ldots\ldots\ldots\ldots (4)$$

$\boldsymbol{\varphi_D}$: Density log-derived porosity.
$\boldsymbol{\rho_{ma}}$**:** Matrix density (dry rock) and in this study = 2.71(g/cm^3) from limestone formation [7].
$\boldsymbol{\rho_b}$: Bulk density recorder by log (gm/cc).
$\boldsymbol{\rho_f}$: The density of the fluid as it is (1.2 g/cm^3) for salty mud in units (g/cm^3) [8].

(2) Neutron log (NPHI Log)

This log is one of the types of porosity logs that measures the amount of hydrogen ion concentration present in the rocks, meaning that the response of the log represents the percentage of the hydrogen content of the fluids inside the formation pores. While the emitted neutrons from a radioactive source towards the formation occur mutual interactions between the neutrons and the hydrogen nucleus, which leads to a loss of energy neutrons [2], (Figures 2,3,4, and 5).

(3) Acoustic or Sonic log (DT Log)

A sonic log is one of the types of porosity logs that measures the time interval of transmission of the compressive sound wave within one foot of the formation ($\boldsymbol{\Delta t}$) and it is measured in units (µsec/ft) [6]. It depends on the nature minerals that formed the rock, the type of fluids inside the pore space, the porosity of the rock, pressure, and temperature [10]. The sonic log is used to determine the porosity of sandstone and carbonate rocks. Where the sonic-derived porosity is measured from eq. (5) [9], (Figures 2,3,4, and 5):

$$\varphi_{sonic} = \frac{\Delta t_{log}-\Delta t_{ma}}{\Delta t_f-\Delta t_{ma}} \qquad \ldots\ldots\ldots\ldots\ldots\ldots\ldots\ldots (5).$$

$\boldsymbol{\varphi_{sonic}}$**:** The sonic-derived porosity.

Δt_{log}**:** The interval of wave travel through the formation is measured from the sonic log recording.
Δt_{ma}**:** The interval of wave travel through the matrix is 47.6 (μsec/ft) for limestone [8].
Δt_f**:** The interval of wave travel through the liquid or fluid is equal to (185/ (μsec/ft) for salt water [8].

(4) Effective and secondary porosities

Effective porosity is the percentage of the volume of the connected pores in a rock model to the volume of the total rock model. It is called effective porosity because it is effective in the fluid's movement and passing them through the rock as it expresses the number of connected pores. Effective porosity is calculated from the eq. (6) [11]:

$$\varphi_{N.D} = \frac{(\varphi_N+\varphi_D)}{2} \dots \qquad \dots\dots\dots\dots\dots\dots (6)$$

$\varphi_{N.D}$**:** Effective porosity (total porosity φt).
φ_N**:** The neutron-derived porosity.

The secondary porosity in general is less than the effective porosity and can be neglected in the most sections of Khasib formation. When secondary porosity has high values, which indicated to the presence of diagenesis processes [12].

The results indicated that the effective porosity rate is very good to excellent for all selected wells (with an average of Kh1: (0- 0.261), Kh2: (0.013- 0.322), and Kh3: (0- 0,296)), (Table (2), and Figures 2, 3, 4 and 5) [13].

Table 2: The average values for calculating the effective porosity for the studied wells.

Unit No.	EB-83	EB-87	EB-92	EB-94
Kh1	0.045- 0.183	0.034- 0.171	0- 0.261	0- 0.222
Kh2	0.041- 0.322	0.087- 0.246	0.032- 0.182	0.013- 0.168
Kh3	0.025- 0.234	0.086- 0.296	0- 0.197	0.011- 0.211

The effective porosity of Khasib Formation in these studied wells is very good to excellent, according to Leverson (1972) [13], and it is equal to the total porosity.

Secondary porosity was calculated using the eq. (7) [11]:

$$SPI = (\varphi_{N.D} - \varphi_{sonic}) \qquad \dots\dots\dots\dots\dots\dots\dots\dots\dots\dots (7).$$

SPI**:** Secondary porosity index.

Its percentage was less than 5% and it is very little or negligible [13].

3.1.3 Calculation of water and hydrocarbon saturation

The water saturation (Sw) is the percentage of the volume of the voids occupied by water to the total volume of the voids in the rock [14]. As for hydrocarbon saturation, it is the remainder of the volume of the voids not occupied with water [15]. The water saturation of the wells was calculated for the unflushed zone (S_W) with the mud filtrate as well as the water saturation in the flushed zone (S_{xo}). The following equations (8 and 9) [16], (Figures 2,3,4 and 5):

$$S_W = (FR_W/R_T)^{1/n} \qquad \dots\dots\dots\dots\dots\dots (8).$$

S_W**:** Water saturation of the unflushed zone (%).
F**:** Formation coefficient. $F = a/\varphi_m$
a: The coefficient of entanglement and its value is (1.0).

m: Noun cementation and its value is (2).
$\boldsymbol{R_W}$**:** Resistivity of water formation (0.027 Ω.m for Khasib Formation), (from Midline oil company).
$\boldsymbol{R_t}$**:** True formation resistivity (read from a log LLD), (Ω.m).
n: An exponent of saturation that ranges between (1.8- 2.5) but is equal to (2) for carbonate rocks.

$$S_{xo} = (FR_{mf}/R_{xo})^{1/n} \ldots \qquad \ldots\ldots\ldots\ldots\ldots\ldots\ldots.. (9).$$

$\boldsymbol{S_{xo}}$**:** Water saturation of the flushed zone (%).
$\boldsymbol{R_{mf}}$**:** Resistivity of mud filtrate at formation temperature (0.05 Ω.m in 66 $C^o$for Khasib Formation), (from Midline oil company).
$\boldsymbol{R_{xo}}$**:** Resistivity flushed zone resistivity (read from a log MSFL), (Ω.m).
To calculate the hydrocarbon saturation (S_h) that can be defined as the movable and residual hydrocarbons through the pore systems, which unfilled with water [15]. Using the eq.(10), to obtain S_h, (Figures 2,3,4, and 5) [17]:

$$S_h = 1 - S_w \ldots \qquad \ldots\ldots\ldots\ldots\ldots\ldots\ldots\ldots (10)$$

$\boldsymbol{S_h}$**:** The hydrocarbon saturation.

3.1.4 Calculation of the total volume and movement of hydrocarbons

It is not sufficient to calculate the water saturation (S_w) for the purpose to estimate the residual hydrocarbon saturation (*ROS*) and the movable hydrocarbon saturation (*MOS*) from the following equations (11 and 12) [18]:

$$ROS = 1 - S_{xo} \ldots \qquad \ldots\ldots\ldots\ldots\ldots\ldots\ldots\ldots (11)$$

ROS**:** Residual oil saturation.

$$MOS = S_{xo} - S_w \qquad \ldots\ldots\ldots\ldots\ldots\ldots\ldots\ldots\ldots (12)$$

MOS**:** Movable hydrocarbons saturation.

(1) Bulk volume analysis

Calculates the total water volume in the flushed zone resistivity (S_{xo}) and unflushed zone (S_w) ranges of drilling mud according to the following the equations (13 and 14) [19]:

$$BV_w = S_w \varphi \qquad \ldots\ldots\ldots\ldots\ldots\ldots\ldots\ldots\ldots.. (13).$$

$$BV_{xo} = S_{xo} \varphi \ldots \qquad \ldots\ldots\ldots\ldots\ldots\ldots\ldots\ldots\ldots (14).$$

$\boldsymbol{BV_w}$**:** Bulk volume water in the unflushed zone.
$\boldsymbol{BV_{xo}}$**:** Bulk volume of water in the flushed zone.
Bulk volume of total hydrocarbons for saturation of the movable oil and the saturation of the (immovable) oil residue and is calculated from eq. (15) [18]:

$$BV_o = S_h \varphi \qquad \ldots\ldots\ldots\ldots\ldots\ldots\ldots\ldots (15).$$

$\boldsymbol{BV_o}$**:** Bulk volume of hydrocarbons.

The space between (BV_w) and (BV_{xo}) represents the volume of producible hydrocarbons (moveable hydrocarbons), and the space between (φ) and (S_{xo} φ) represents the volume of hydrocarbons suspended in the walls of the voids (residual hydrocarbons), and the space between (φ) and (S_w φ) represents the volume of total hydrocarbons (BV_o) [20], (Figures 2, 3, 4, and 5).

In the well (EB-83), it is noticed that ($ROS > MOS$) is present in the upper part of the formation, which is evidence of poor permeability, but that ($ROS < MOS$) is present in the middle and lower regions, which is evidence of high permeability. The ($ROS > MOS$) is present in all areas of the formation in the wells (EB-87 and EB-92), which is evidence of low permeability.

In addition, the (ROS < MOS) is present in all areas of the formation in the well (EB-94), which is evidence of high permeability.

3.1.5 Applications obtained from equations and cross plots

One of the crucial applications that can be used to precisely calculate porosity values and diagnose lithology and minerals is the use of a cross-plot to read specific porosity logs. These profiles are useful only in the presence of limestone, sandstone, and dolomite, but they are inaccurate in the presence of clays and some other abnormal minerals [21], and among these applications are the following:

(1)Neutron- Density cross plot for identification of lithology

Porosity logs are affected by the formation's rocky content, clay content, and the presence of gas. These logs are used interconnected rather than singly [21,22]. The values of the neutron log (φ_N)and the density log (φ_D) were represented on the profile for the selected wells within Khasib formation in the East Baghdad field [19]. All points are located in the limestone with dolomite and less sandstone intrusions, with a density ranging [EB-83= (2.15- 2.8 g/cm^3), EB-92= (2- 2.75 g/cm^3), and EB-94= (2.15- 2.75 g/cm^3)] (Figures 6, 7, 8 and 9). Regarding the well (EB-87), all locations are situated inside the limestone range with dolomite intrusions that range in density (2.25 - 2.75 g/cm^3) (Figure 7).

3.1.6 Well correlation

It is important to show the logs correlation of the drilled wells in order to assess the geometrical shape of Khasib Formation surfaces (upper and lower), based on the main logs such as gamma-ray, sonic, density, neutron, and resistivity, (Figure 10). Actually, the three rock units Kh1, Kh2, and Kh3 of the four wells EB-83, EB-87, EB-92, and EB-94 were matched. It was found that the formation is confined to two cap rocks from the top Tanuma Formation with the shale and from the bottom Kifl Formation with anhydrite.

The best reservoir unit for oil storage in terms of maximum values of porosity, water saturation, and diagenesis processes and the microfacies analysis is the unit (Kh 2), while, in terms of porosity, it is found that Kh 3 unit is the best in all the studied wells.

4. Conclusions

1. It was found that the effective porosity is the dominant porosity in the Khasib formation, according to porosity logs analyses (density, neutron, and sonic), ranged from 0.0 to 32 % in all well and classified as very good to excellent porosity.
2. The stratigraphic borders of the Khasib Formation were identified using porosity, resistance and gamma rays logs. The Tanuma Formation is at the top and the Kifl Formation is at the bottom conformably. Moreover, the formation consists of two cap rocks, one from the bottom Kifl Formation with anhydrite and the other from the top Tanuma Formation with shale.
3. The lithology of Khasib Formation consists of limestone through the cross-plot between the total density and the neutron to elicit the lithology.
4. Kh 2 unit is the best oil reservoir unit in all selected wells in terms of porosity, water saturation, diagenesis processes and microfacies analysis.
5. The maximum effective porosity (0.32%) value in the unit (Kh2) well (EB-83), is the best well in terms of oil productivity.

Acknowledgements:

The authors would like to thank the Department of Petroleum Geology and Minerals, College of Science, University of Diyala, for their help during this work. The authors acknowledge both unknown reviewers for their constructive suggestions and comments. Sincere thanks to Dr. Aiad Ali Hussain Al-Zaidyfor guiding and helping during the study.

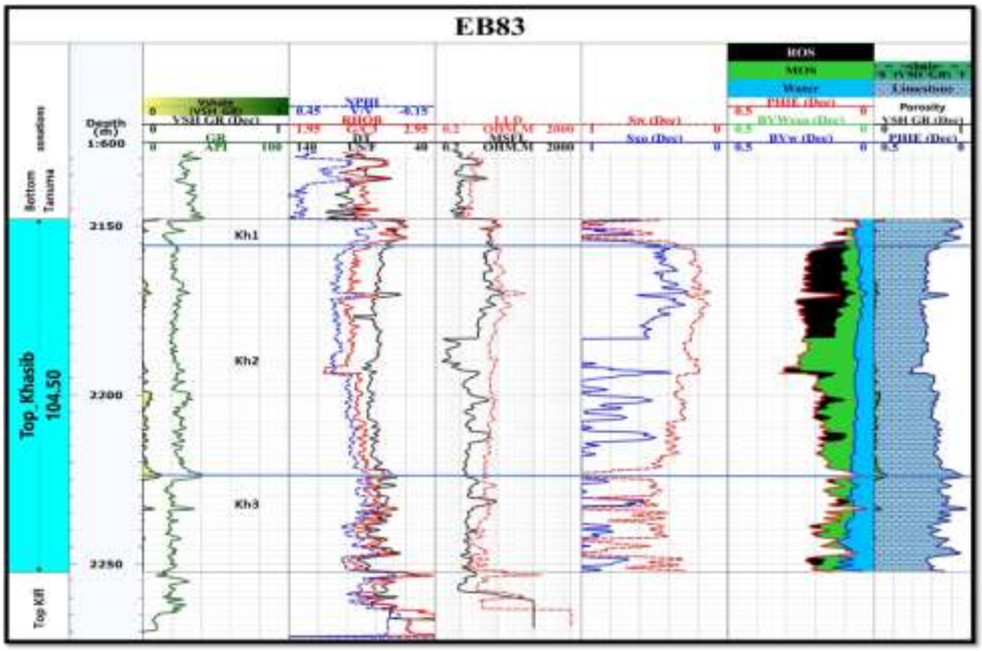

Figure 2: Computer Processed Interpretation (CPI) of well **EB-83**.

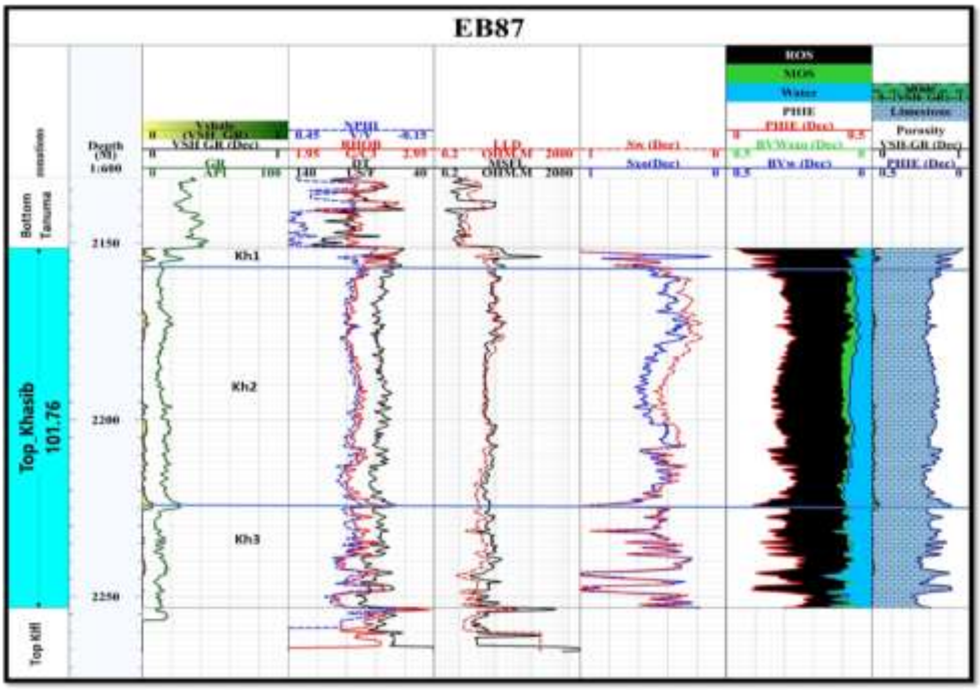

Figure 3: Computer Processed Interpretation (CPI) of well **EB-87**.

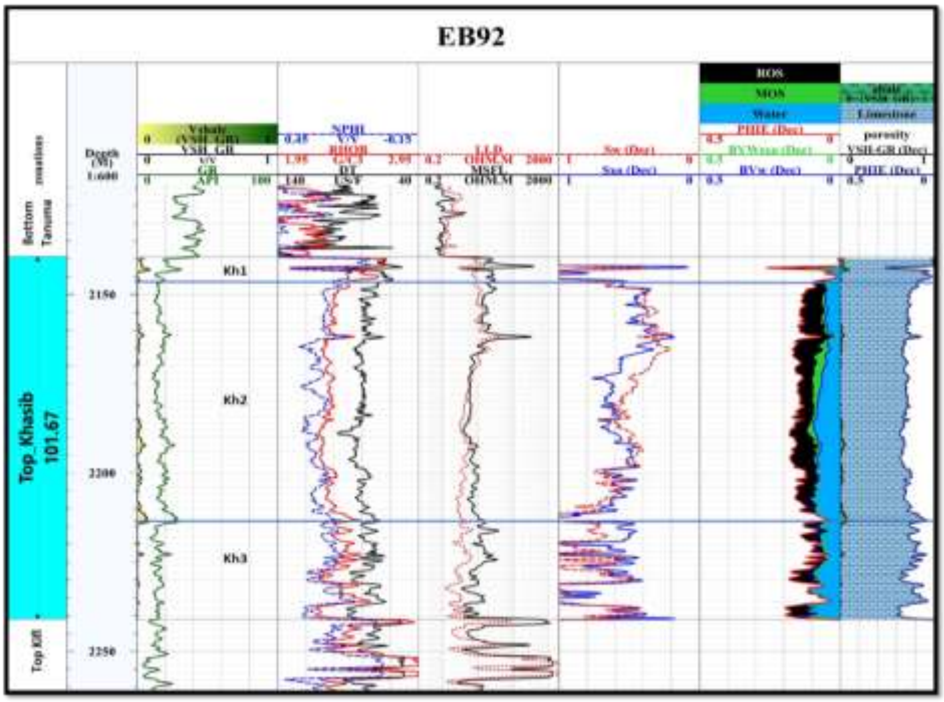

Figure 4: Computer Processed Interpretation (CPI) of well **EB-92**.

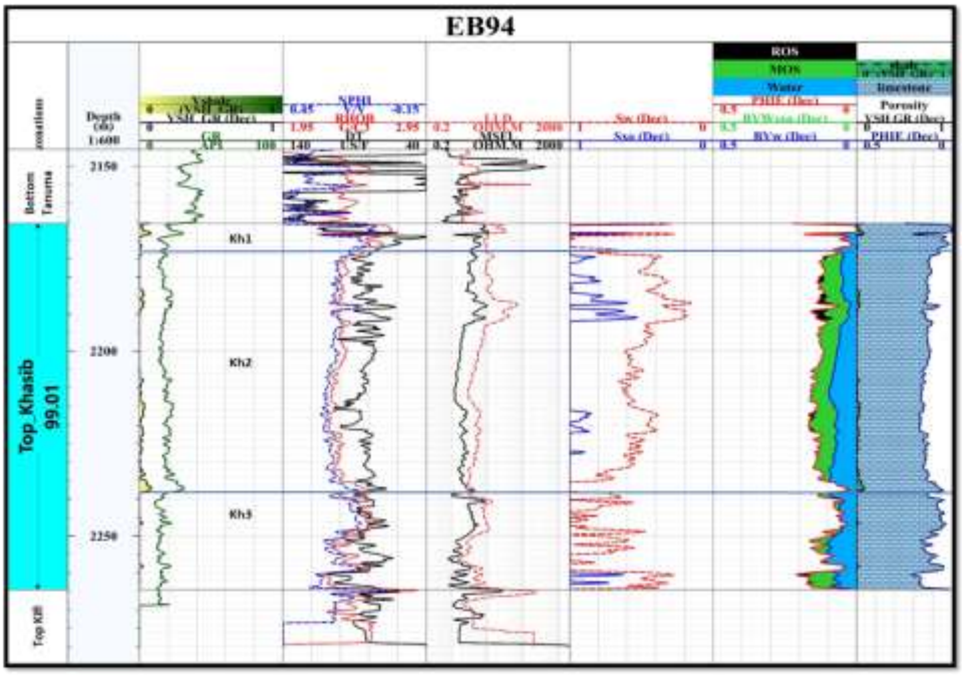

Figure 5: Computer Processed Interpretation (CPI) of well **EB-94**.

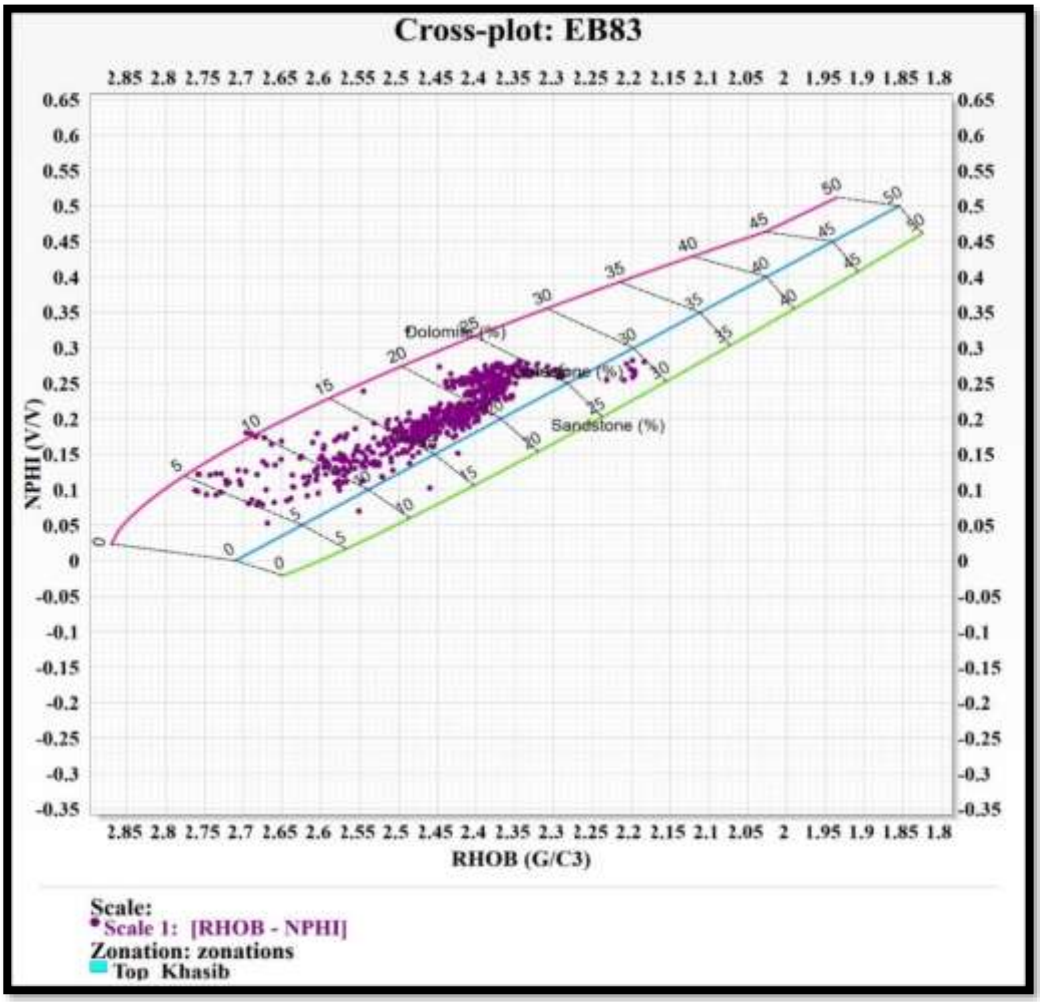

Figure 6: The cross plot of φ_N and φ_D for well **EB-83**.

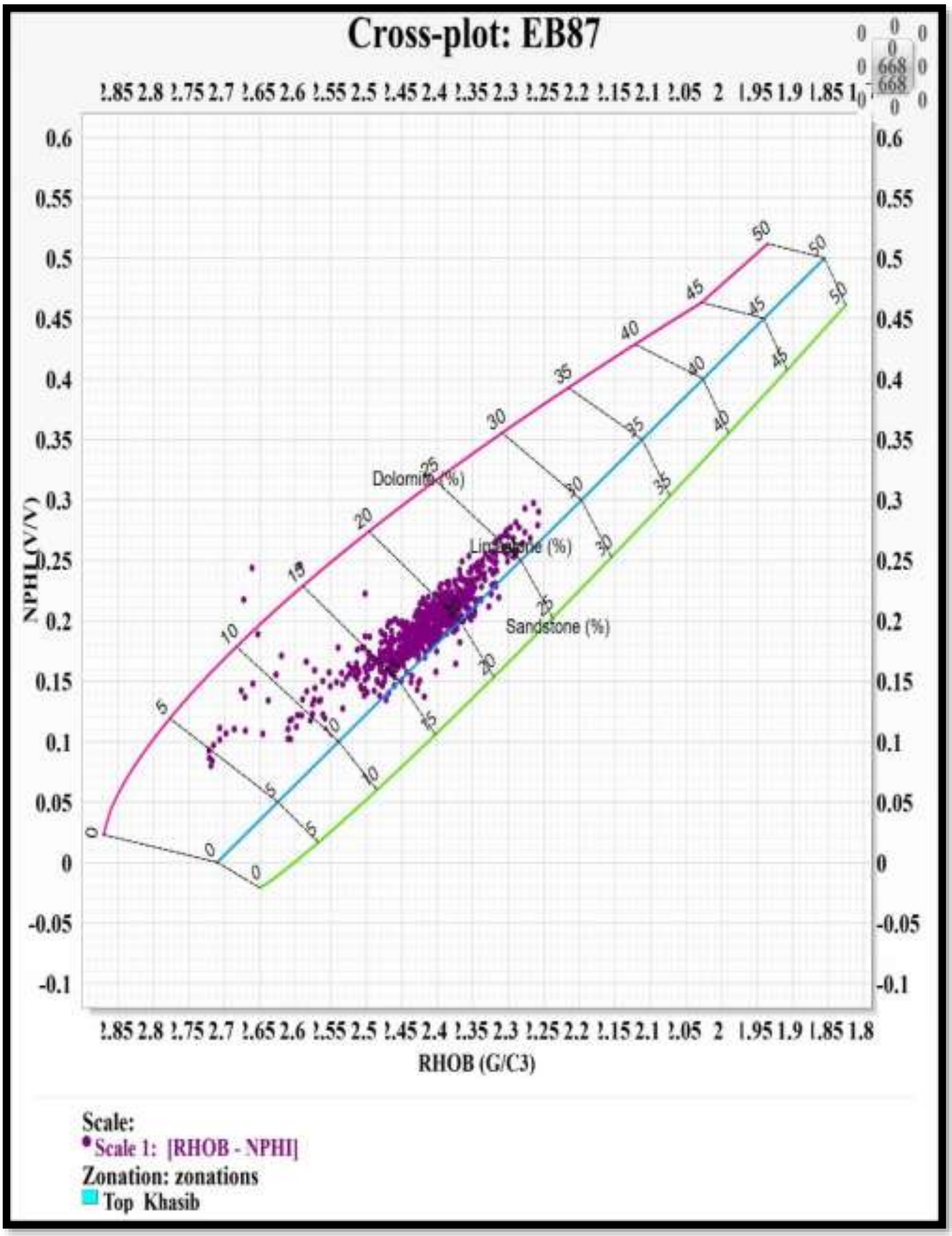

Figure 7: The cross plot of φ_N and φ_D for well **EB-87**.

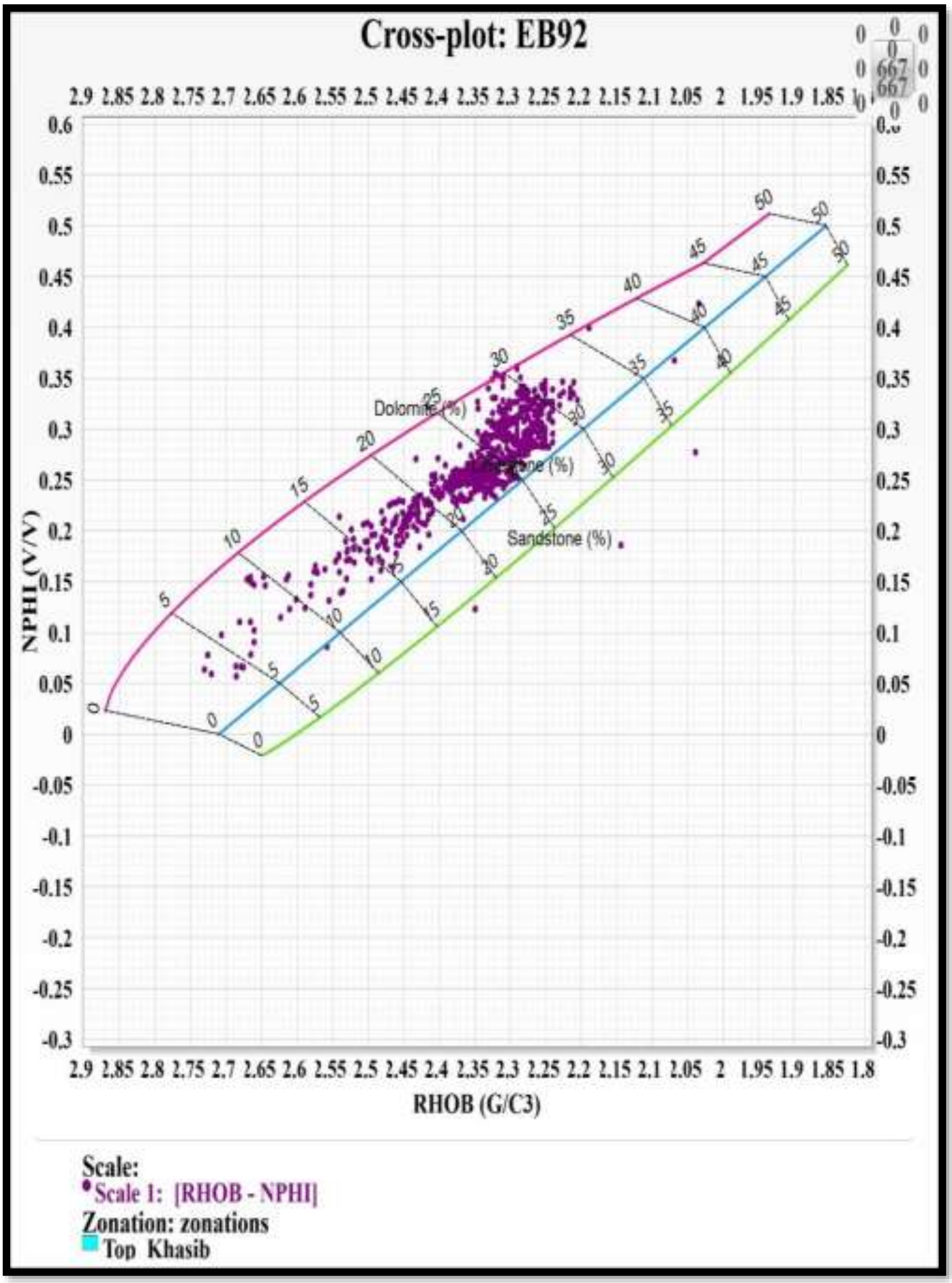

Figure 8: The cross plot of φ_N and φ_D for well **EB-92**.

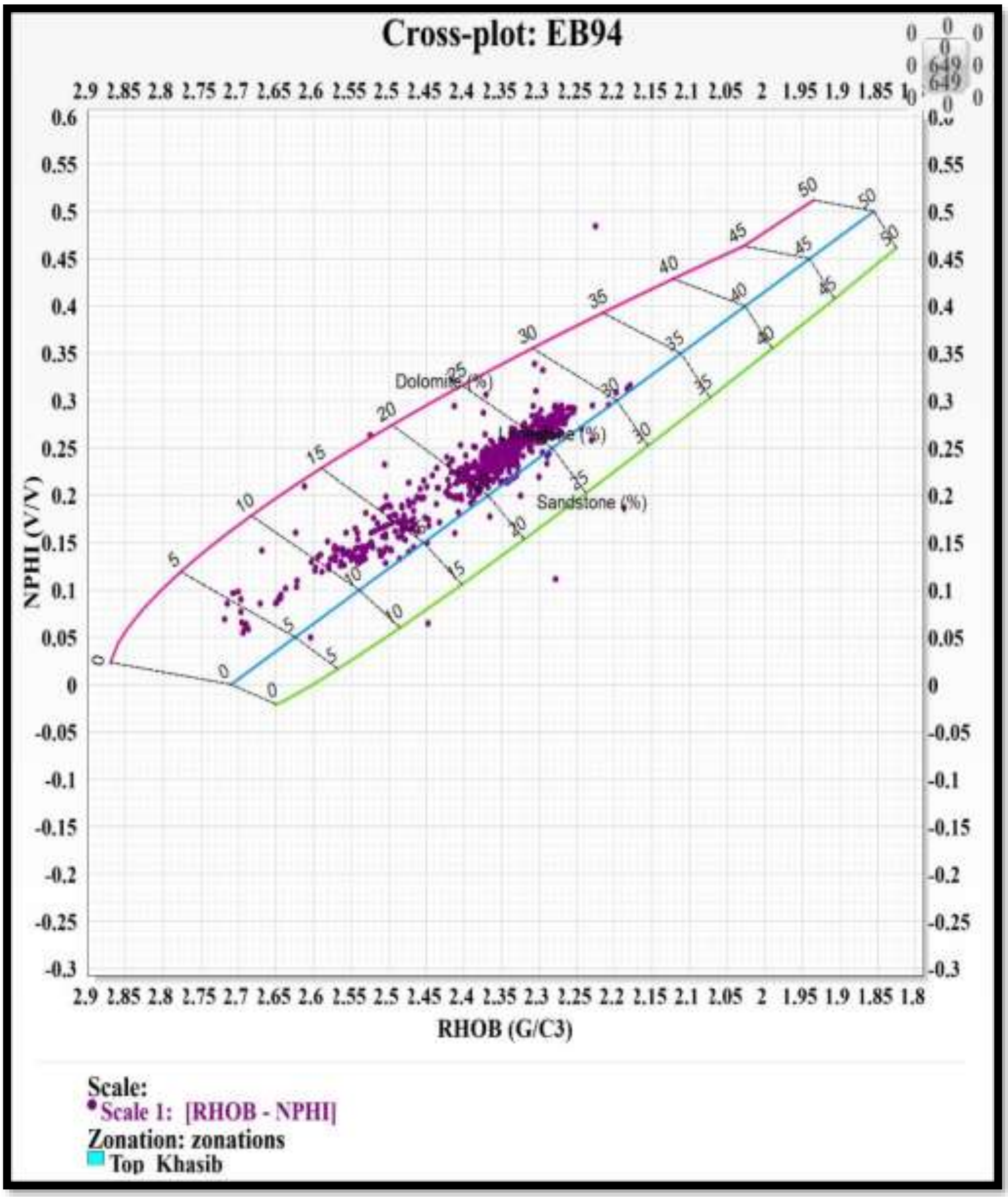

Figure 9: The cross plot of φ_N and φ_D for well **EB-94**.

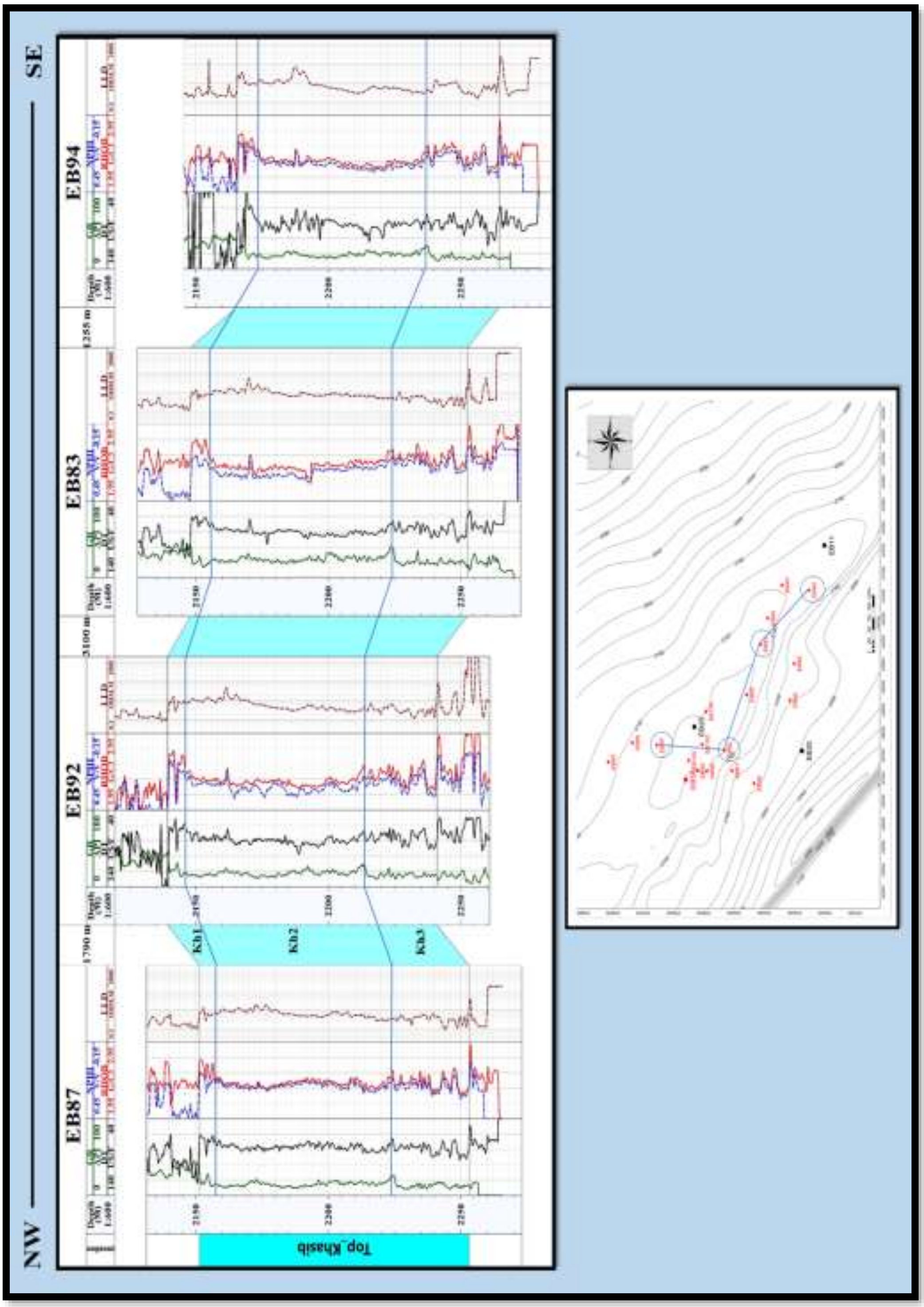

Figure 10: Well logs correlation in East Baghdad oil field showing Khasib tops and based on the selected wells.

References

[1] R. C. Van Bellen, H. V. Dunnington, R. Wetzel, and D. Morton, "Lexique Stratigraphique International,". *Asie*, *Iraq*, vol. 3, no. 10a, 113 p., 1959.

[2] G. Asquith, and C. Gibson, "Basic Well Log Analysis for geologists: Methods in Exploration Serise," *American Association of Petroleum Geologist*, 216 p., 1982.

[3] Schlumberger, "Log Interpretation Manual Applications," Houston, Schlumberger Well Services, Inc, vol. 2, 116 p., 1974.

[4] V. V. Larionov, "Borehole Radiometry," Moscow, U.S.S.R., Nedra. 233 p., 1969.
[5] A. M. H. Altameemi, and A. Alzaidy, "Formation Evaluation by using Well Logging of Mishrif Formation in the Noor Oil Field, Southeast Iraq," *Iraqi Journal of Science*, vol. 59, no. 1A, pp. 144-155, 2018.
[6] Baker Hughes INTEQ, "Petroleum Geology," workbook, Training and Development. United States of America, 254 p., 1999.
[7] D. J. Hartman, "Gupco petrophysics workshop," Cairo, Egypt. 1997
[8] Schlumberger, "Log Interpretation Principles," vol. 1, New York, 112 p., 1972.
[9] M. R. Wyllie, A. R. Gregory and H. F. Gardner. "An experimental investigation of the factors affecting elastic wave velocities in porous media," *Geophysics*, vol. 23, pp. 459-493, 1958.
[10] R.C. Selley, "Elements of petroleum Geology," Academic Press, London, 467 p., 1998.
[11] Schlumberger, "Log Interpretation Charts," Houston, Schlumberger wireline testing, 193p., 1997.
[12] Al-maini, A. H., and Mad'hat, E. N, "Well Log Analysis and Interpretation for Khasib, Tanuma, and Sa'di formations for Halfaya Oil Field in Missan Govenorate-Southern Iraq," *Iraqi Journal of Science*, vol. 59, no. 1C, pp. 520-533., 2018.
[13] L. A. Leverson, "Geology of petroleum," Second edition, Freeman and W. H. Company Pub., San Francisco and London 724 p., 1972.
[14] M. H. Khayouka, "Physical Interpretations," Dar Al-Kutub, University of Mosul, 376 p., 1991.
[15] O. Serra, "Fundamentals of well log interpretation," The Acquisition of logging data. Development in petroleum science, Elsvier, Amsterdam, vol.1, no. 15A, 440 p., 1984.
[16] G. E. Archie, "The Electrical Resistivity Log as an Aid in Determinig Some Reservoir Characteristics," AIME, vol.146, 45 p., 1942.
[17] Schlumberger, "Log Interpretation Principles Application, New York. 160 p., 1987.
[18] G. Asquith and D. Krygowskti, "Basic Well Log Analysis," Second edition, *American Association of Petroleum Geologist*, Methods in Exploration Series 16. 244 p., 2004.
[19] A. W. Schmidt, A. G. Hand, J. D. Yumker and E. C. Kilgore, "Application of the coriband technique in complex lithologies," SPWIA sump. 1971.
[20] Schlumberger, "Well Evaluation conference, India, 263 p., 1984.
[21] F. N. Al-Saadouni and A. M. Aqrawi, "Createaceous sequence stratigraphy and petroleum potential of the Mesopotamian basin, Iraq," Society of Sedimentary Geology, SEPM, pp. 315-334., 2001.
[22] B. A. Al-Juraisy and M. H. A. Al-Majid, "Importance of Velocity Deviation Technique and Negative Secondary Porosity in Detection of Hydrocarbon Zones in Khasib Formation,' East Baghdad Oil Field," *The Iraqi Geological Journal*, vol. 54, no. 2E, pp.86-103., 2021.